

tility caused by genetic factors and drug toxicity.

Recently, transgenic mice were produced by retroviral transduction of male germline stem cells (32). However, the efficiency and the definition of integration of exogenous genes into the genome remain to be improved. It is very difficult to transfer genes into primary cultures of spermatogonia and impossible to select them with drugs in vitro. Use of the spermatogonial cell line may resolve current challenges with primary cultures of isolated spermatogonia and may greatly increase the success and efficiency of generating transgenic mice.

References and Notes

1. M. Starz-Gaiano, R. Lehmann, *Mech. Dev.* **105**, 5 (2001).
2. P. P. Tam, M. H. Snow, *J. Embryol. Exp. Morphol.* **64**, 133 (1981).
3. P. J. Donovan, D. Stott, L. A. Cairns, J. Heasman, C. C. Wylie, *Cell* **44**, 831 (1986).
4. A. McLaren, *Mol. Cell. Endocrinol.* **163**, 3 (2000).
5. M. Dym, *Proc. Natl. Acad. Sci. U.S.A.* **91**, 11287 (1994).
6. N. Ravindranath *et al.*, *Endocrinology* **138**, 4026 (1997).
7. H. W. Lee *et al.*, *Nature* **392**, 569 (1998).
8. W. C. Hahn *et al.*, *Nature* **400**, 464 (1999).
9. C. P. Morales *et al.*, *Nature Genet.* **21**, 115 (1999).
10. M. Dym *et al.*, *Biol. Reprod.* **52**, 8 (1995).
11. A 3441-base pair (bp) EcoRI/EcoRI fragment carrying 3395 bp of full-length murine telomerase reverse transcriptase (mTERT) cDNA was obtained from pGRN188 and subcloned into EcoRI site in a retrovirus vector pLXSN (Clontech). The orientation for expressing sense mTERT by 5' LTR was checked by digestion with Xho I. Expression of Neo<sup>r</sup> was driven by SV40 early promoter. Viruses were harvested from supernatants of transfected Phoenix packaging cells.
12. W. S. Pear *et al.*, *Proc. Natl. Acad. Sci. U.S.A.* **90**, 8392 (1993).
13. M. Ruggiu *et al.*, *Nature* **389**, 73 (1997).
14. H. R. Schöler, S. Ruppert, N. Suzuki, K. Chowdhury, P. Gruss, *Nature* **344**, 435 (1990).
15. Total RNA was isolated and cDNA synthesis was carried out with random hexamers. RT-PCR amplification of Oct-4 used primers 5'-AGCTGCTGAAGCA-GAAGAGG-3' and 5'-GGTTCCTCATTGTGTCGGCT-3' (94°C for 35 s, 55°C for 30 s, and 72°C for 45 s; 30 cycles). The size of the RT-PCR product was 207 bp. Primers for RT-PCR amplification of protamine-2 were 5'-GAGCGCTAGAGGACTATGG-3' and 5'-GCAAGTGACTTCCTGGCTC-3' (94°C for 30 s, 58°C for 30 s, and 72°C for 45 s; 35 cycles). The product was a 282-bp DNA fragment.
16. M. Pesce, M. K. Gross, H. R. Schöler, *Bioessays* **20**, 722 (1998).
17. D. G. de Rooij, J. A. Grootegoed, *Curr. Opin. Cell Biol.* **10**, 694 (1998).
18. H. Ohta, K. Yomogida, K. Dohmae, Y. Nishimune, *Development* **127**, 2125 (2000).
19. P. Blume-Jensen *et al.*, *Nature Genet.* **24**, 157 (2000).
20. H. Kissel *et al.*, *EMBO J.* **19**, 1312 (2000).
21. Z. G. Liang, J. A. Shelton, E. Goldberg, *J. Exp. Zool.* **240**, 377 (1986).
22. Single-letter abbreviations for amino acid residues are as follows: A, Ala; C, Cys; D, Asp; E, Glu; F, Phe; G, Gly; H, His; I, Ile; K, Lys; L, Leu; M, Met; N, Asn; P, Pro; Q, Gln; R, Arg; S, Ser; T, Thr; V, Val; W, Trp; and Y, Tyr.
23. T. Nakanishi *et al.*, *FEBS Lett.* **449**, 277 (1999).
24. S. Kashiwabara, Y. Arai, K. Kodaira, T. Baba, *Biochem. Biophys. Res. Commun.* **173**, 240 (1990).
25. Acr3-EGFP-pcDNA3.1/Zeo(-) was created by subcloning the Xba I/Hind III fragment of Acr3-EGFP [containing acrocin promoter, the fused peptide MVEMLPTVAVLVLAVSVVA-KDNTT-EGFP (22), and bovine growth hormone polyadenylate from pUC19/Acr3-EGFP] into pcDNA3.1/Zeo(-).

26. P. P. Reddi, C. J. Flickinger, J. C. Herr, *Biol. Reprod.* **61**, 1256 (1999).
27. P. Mali *et al.*, *Reprod. Fertil. Dev.* **1**, 369 (1989).
28. X. Meng *et al.*, *Cancer Res.* **61**, 3267 (2001).
29. M. C. Hofmann, R. A. Hess, E. Goldberg, J. L. Millan, *Proc. Natl. Acad. Sci. U.S.A.* **91**, 5533 (1994).
30. M. J. Wolkowicz *et al.*, *Biol. Reprod.* **55**, 923 (1996).
31. T. R. Yeager, R. R. Reddel, *Curr. Opin. Biotechnol.* **10**, 465 (1999).

32. M. Nagano *et al.*, *Proc. Natl. Acad. Sci. U.S.A.* **98**, 13090 (2001).
33. We thank M. Okabe for pUC19/Acr3-EGFP, P. Moens for antibody to SCP3, and R. A. DePinho for pGRN188. Supported in part by NIH grant HD-36483.

22 April 2002; accepted 12 June 2002  
 Published online 20 June 2002;  
 10.1126/science.1073162  
 Include this information when citing this paper.

## Systematic Identification of Pathways That Couple Cell Growth and Division in Yeast

Paul Jorgensen,<sup>1,2\*</sup> Joy L. Nishikawa,<sup>1,2\*</sup> Bobby-Joe Breitreutz,<sup>2</sup> Mike Tyers<sup>1,2†</sup>

Size homeostasis in budding yeast requires that cells grow to a critical size before commitment to division in the late prereplicative growth phase of the cell cycle, an event termed Start. We determined cell size distributions for the complete set of ~6000 *Saccharomyces cerevisiae* gene deletion strains and identified ~500 abnormally small (*whi*) or large (*lge*) mutants. Genetic analysis revealed a complex network of newly found factors that govern critical cell size at Start, the most potent of which were Sfp1, Sch9, Cdh1, Prs3, and Whi5. Ribosome biogenesis is intimately linked to cell size through Sfp1, a transcription factor that controls the expression of at least 60 genes implicated in ribosome assembly. Cell growth and division appear to be coupled by multiple conserved mechanisms.

Size homeostasis, whereby cell growth is coupled to cell division, is a universal but poorly understood feature of cell cycle control (1). In the budding yeast *S. cerevisiae*, coordination of division with growth occurs at Start, where cells must reach a critical cell size to enter the cell cycle (2–4). This size threshold increases in proportion to cell ploidy and nutrient status (5, 6). In fission yeast, unicellular algae, mouse fibroblasts, and human lymphoid cells, entrance into the DNA replication phase of the cell cycle (S phase) also requires that cells obtain a critical cell volume, as modulated by ploidy and extracellular signals (7–11). Recently, a signaling pathway comprising phosphoinositide-3'-kinase, the phosphoinositide phosphatase PTEN, Akt/protein kinase B (PKB), and ribosomal S6 kinase (S6K) has been implicated in cell size control in flies and mice (1, 12–14).

Mutations that accelerate cell division relative to cell growth result in a small cell size, referred to as a Wee or Whi phenotype in

fission yeast and budding yeast, respectively. Such mutants have provided key insights into cell cycle control (7, 15–18). Two *whi* mutants, *WHI1-1* (or *CLN3-1*) and *whi3*, have a reduced critical cell size at Start. *WHI1-1* is a hypermorphic allele of *CLN3*, which encodes a cyclin that activates the cyclin-dependent kinase Cdc28 to cue events at Start (15–17, 19), whereas Whi3 is an RNA binding protein that sequesters the *CLN3* transcript into an inactive state (18, 20). In the late prereplicative growth phase of growth (G<sub>1</sub>), the Cln3-Cdc28 kinase and another protein of unknown function, Bck2, impel the SCB binding factor (SBF) (Swi4-Swi6) and MCB binding factor (MBF) (Mbp1-Swi6) transcription factor complexes to drive the expression of a suite of ~120 genes, including the G1 cyclins *CLN1* and *CLN2* (19, 21–23). Cln1-Cdc28 and Cln2-Cdc28 activity triggers key events at Start, including bud emergence, spindle pole body duplication, and elaboration of Clb-Cdc28 activity, which is needed for DNA replication (3).

Despite the insights gleaned from analysis of *whi* mutants, few such mutants have been characterized because of the difficulties inherent in cloning genes that affect cell size (16). The recent construction of a complete set of yeast open reading frame (ORF) deletion strains allowed us to survey 4812 viable haploid deletion strains for alterations in the cell size distributions of exponentially grow-

<sup>1</sup>Department of Medical Genetics and Microbiology, University of Toronto, Toronto, Ontario, Canada M5S 1A8. <sup>2</sup>Program in Molecular Biology and Cancer, Samuel Lunenfeld Research Institute, Mount Sinai Hospital, Toronto, Ontario, Canada M5G 1X5.

\*These authors contributed equally to this work.  
 †To whom correspondence should be addressed. E-mail: tyers@mshri.on.ca

REPORTS

ing cultures (24–26). A wide range of size distributions was observed: The smallest strains, such as *sfp1Δ* and *sch9Δ*, had a median cell volume ~40% smaller than wild-type cells, and the largest strains, such as *cdc10Δ*, had a median cell volume >70% larger than wild-type cells (Fig. 1A). We clustered the size distributions with standard algorithms and represented each as a one-dimensional color plot (26–29). Because cell

size distributions reflect many parameters, clustering of such distributions can reveal genes with shared functions (fig. S1). This clustering also separated small (*whi*) and large (*lge*) cell size haploid deletion mutants from the majority of other viable mutants, whose size distributions were indistinguishable from wild-type controls (Fig. 1B). We classified the largest 5% of deletion strains as *Lge* and the smallest 5% as *Whi* (26).

The functions of genes that affect cell size fell into a number of distinct categories. All of the known Start regulators with pronounced cell size defects were isolated as *lge* (*swi4Δ*, *swi6Δ*, *cln3Δ*, and *bck2Δ*) or *whi* (*whi3Δ*) deletion strains. Debilitation of any process important for cell cycle progression but not growth should, in principle, lead to an increase in cell size (4). Indeed, the predominant class of *lge* mutants corresponded to genes involved in cell cycle progression (fig. S2). Large cell size also resulted from perturbation of the actin cytoskeleton, secretory pathways, translation components, and global regulators of RNA Pol II transcription, all of which can directly or indirectly affect cell cycle progression. The majority of *whi* strains lacked components of the ribosome or the mitochondrial respiratory apparatus (fig. S2) (26). The small cell size of these mutants is probably a consequence of slow growth rate, which causes cells to accumulate in G<sub>1</sub> phase. Gene deletions that attenuated translation, ribosome biogenesis, and glucose signaling also diminished cell size, as did 33 candidate *WHI* genes of unknown function.

Given that some essential genes might regulate cell size and that Start regulators are often dosage sensitive (15, 16), we sized the complete set of 1142 diploid strains heterozygous for an essential gene deletion (fig. S1). Heterozygous diploid strains were increased up to ~40% (*rpt2Δ/RPT2*) or decreased down to ~15% (*cdc24Δ/CDC24*) in median cell size. Haploinsufficient *lge* mutants corresponded to components of the 26S proteasome, components of a  $\gamma$ -tubulin complex, genes involved in ribosome biogenesis, and several other processes, whereas haploinsufficient *whi* mutants corresponded to factors involved in ribosome biogenesis, nucleolar function, and ribosomal subunits (fig. S2).

The ~500 haploid deletion strains with size distributions distinct from those of wild-type cells required additional tests to reveal the genes with direct roles in cell size control at Start. To determine which of the 249 *lge* strains are perturbed for Start progression, we tested for synthetic lethal interactions with known activators of Start. For example, *CLN3* and *BCK2* act in parallel pathways such that *cln3Δ bck2Δ* double mutants are not viable due to G<sub>1</sub> arrest (21), whereas *cln3Δ swi4Δ* and *bck2Δ swi4Δ* double mutants have growth defects in progression through Start (21, 23). We subjected the entire set of 249 *lge* strains to synthetic genetic array (SGA) analysis to systematically screen for genetic interactions with *cln3Δ*, *bck2Δ*, and *swi4Δ* (26, 30). SGA detected 23 candidate genetic interactions, 12 of which were confirmed by direct tetrad analysis (Fig. 2A). In addition to known interactions, *bck2Δ* and *cln3Δ* exhibited a synthetic growth defect only with deletion of *SST2*, a negative regulator of the mating pathway (31). In contrast, *swi4Δ*

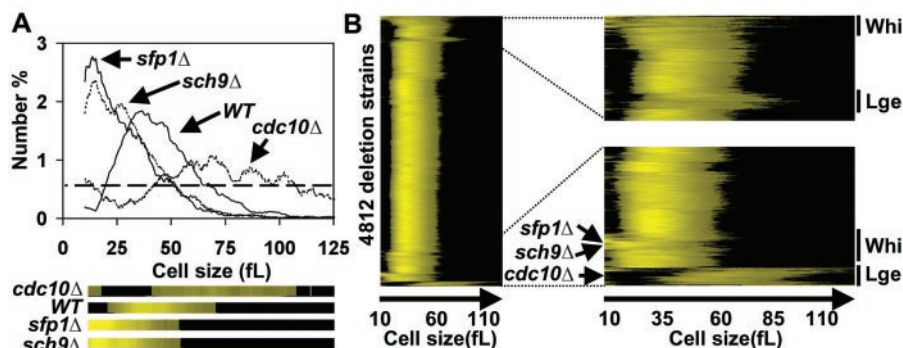
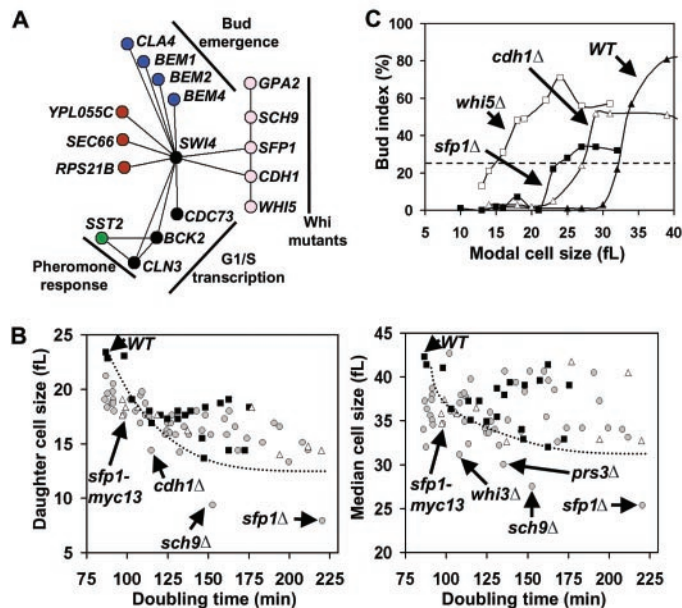


**Fig. 1.** A systematic survey of cell size mutants in *S. cerevisiae*. (A) Cell size distributions for a wild-type (WT) strain as compared to two of the smallest deletion strains, *sfp1Δ* and *sch9Δ*, as well as one of the largest strains, *cdc10Δ*. Distributions are visualized as colored strips, in which all size bins above an arbitrary number % threshold of 0.5% (dotted line) are colored with an intensity proportional to number %. (B) Hierarchical clustering of cell size distributions of 4812 viable haploid deletion strains revealed clusters of strains with *Whi* and *Lge* phenotypes. Sections of the dendrogram containing prominent *Whi* and *Lge* clusters are magnified.

**Fig. 2.** Characterization of novel regulators of Start. (A) Genetic interactions with deletions of the known Start regulators *SWI4*, *CLN3*, and *BCK2* revealed a network of Start activators. Confirmed synthetic genetic interactions (12) between *lge* strains (*cdc73Δ*, *sst2Δ*, *sec66Δ*, *rps21bΔ*, *yp1055cΔ*, *cla4Δ*, *bem1Δ*, *bem2Δ*, and *bem4Δ*) and *swi4Δ*, *cln3Δ*, and *bck2Δ* are represented by lines. Deletion strains are represented by colored nodes: G<sub>1</sub>-S transcription (black), bud emergence (blue), pheromone signaling (green), or other processes (red). Synthetic genetic interactions (Fig. 4A) were also discovered between several *whi* mutants (*gpa2Δ*, *sch9Δ*, *sfp1Δ*, *cdh1Δ*, and *whi5Δ*) and *swi4Δ* (pink nodes). (B) The *Whi* phenotype of 25 deletion strains is not solely attributable to slow growth rate. A plot of doubling time versus cell size for two WT strains and 18 ribosomal gene deletion strains (solid squares) was used to establish a baseline correlation between doubling time and small cell size (dotted line). Another 61 *whi* strains (gray circles) are plotted, including 10 *whi* strains with deletions in genes whose products form part of a nucleolar network (open triangles). The 25 strains that partially uncouple growth from division fall on or below the baseline fitted to the smallest ribosomal gene deletion strains. (C) *WHI5*, *CDH1*, and *SFP1* are negative regulators of Start. Early G<sub>1</sub>-phase daughter cells were isolated by centrifugal elutriation, released into glucose medium, and monitored for bud emergence. In plots of bud index versus modal cell size, Start was defined as 25% budded (19).



and *cln3Δ* exhibited a synthetic growth defect only with deletion of *SST2*, a negative regulator of the mating pathway (31). In contrast, *swi4Δ*

REPORTS

exhibited synthetic genetic interactions with *lge* strains defective in bud emergence (*cla4Δ*, *bem1Δ*, *bem2Δ*, and *bem4Δ*), Start-specific transcription (*cln3Δ*, *bck2Δ*, and *cdc73Δ*), a 40S ribosome component (*rps21BΔ*), and a secretory pathway component (*sec66Δ*). Synthetic lethality was also observed with a deletion of an uncharacterized gene, *YPL055C*, a candidate activator of Start that we named *LGE1*.

To identify potential repressors of Start, we characterized 61 haploid *whi* strains that were not directly compromised in ribosomal or respiratory function. Deletion of genes that regulate Start would be expected to have a greater effect on cell size than could be explained by any associated effects on the rate of cell growth (4, 32). Doubling time was plotted against both median and daughter cell size for the 61 *whi* mutants and, as controls, 2 wild-type and 18 ribosomal gene deletion strains (Fig. 2B). The distribution of doubling time versus cell size for the wild-type strains and the smallest of the ribosomal gene deletion strains established a baseline correlation between growth rate and cell size. Potential negative regulators of Start, represented by 25 *whi* strains, fell on or below this baseline. Of these, only a few have been previously implicated in cell cycle control: *WHI3* encodes a negative regulator of *CLN3* (18, 20), and *CDH1* encodes an activator of the anaphase promoting complex/cyclosome (APC/C), which maintains G<sub>1</sub> phase in fission yeast and flies (33). Two of the smallest strains isolated in the initial screen, *sfp1Δ* and *sch9Δ*, fell well below the baseline (Fig. 2B). *SFP1* encodes a predicted zinc finger transcription factor with a suggested role in the response to DNA damage and the G<sub>2</sub>-to-mitosis (M) phase transition (34). The small cell size of *sfp1Δ* strains had been previously noted but not characterized (34). A fortuitous hypomorphic allele of *SFP1*, created by addition of an epitope tag *sfp1-myc13*, conferred a small cell size with only a marginal increase in doubling time (Fig. 2B). *Sch9* is 49% identical to human Akt1 in the COOH-terminal kinase domain and has been implicated in the control of longevity and stress resistance, as have its metazoan counterparts (14, 35). *SCH9* is also a haploinsufficient *whi* mutant, suggesting it may be a dosage-dependent repressor of Start (see Fig. 3C).

We tested the panel of 25 *whi* mutants for Start-related phenotypes (Table 1). Three mutants, *whi3Δ*, *yor083wΔ*, and *ykr020wΔ*, were resistant to mating pheromone, a phenotype associated with premature traversal of Start (16, 17, 20); therefore, we renamed *YOR083W* and *YKR020W* as *WHI5* and *WHI6*, respectively. To confirm the effects on Start of three potent *whi* mutations, we directly measured their critical cell size, as operationally defined by the cell volume at which bud emergence occurs. Early G<sub>1</sub>-phase daughter cells from wild-type, *whi5Δ*,

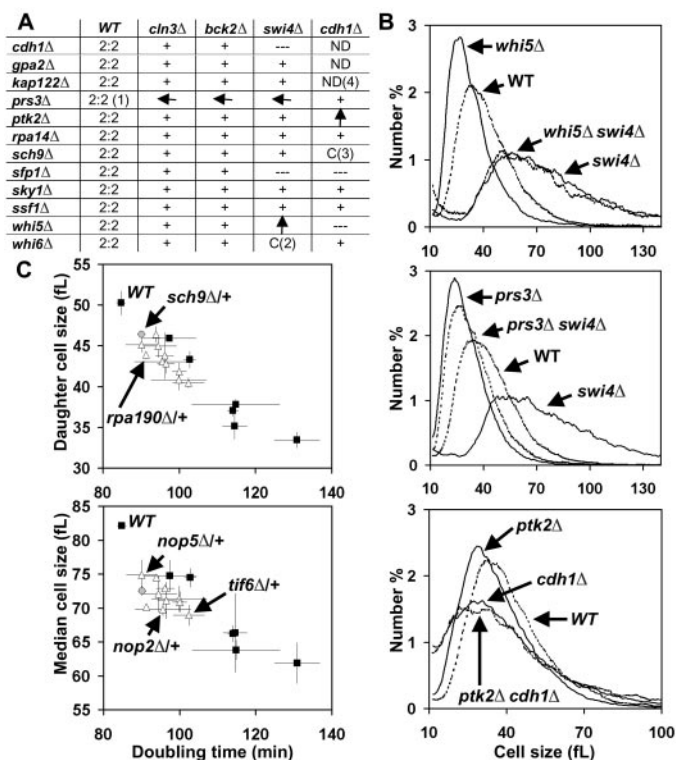
*cdh1Δ*, and *sfp1Δ* cultures were isolated by centrifugal elutriation (19, 26), and progression through Start was monitored by bud index (Fig. 2C). A *whi5Δ* strain passed Start after growing to just 15 fl, half the critical cell size of congenic wild-type cells, which budded at 32 fl. Reductions in critical cell size were also observed in *sfp1Δ* and *cdh1Δ* strains, which budded at 23 fl and 27 fl, respectively. In each *whi* strain tested, the onset of *RNR1* transcription was accelerated as compared to wild-type strains (36). Therefore, *WHI5*, *CDH1*, and *SFP1* encode novel repressors of Start that likely act upstream of SBF and MBF.

To elucidate connections between newly found Start repressors and known pathways, we performed 58 pairwise matings of 12 of the 25 *whi* mutants in Table 1 to wild-type, *cln3Δ*, *bck2Δ*, *swi4Δ*, and *cdh1Δ* strains (26). Seven *whi* mutants showed only additive effects on cell size in combination with the known Start regulators. Epistatic size interactions were observed with *whi5Δ*, *prs3Δ*, and *ptk2Δ*, and more complicated interactions were observed with *whi6Δ* and *sch9Δ* (Fig. 3A). The size distribution of the *whi5Δ swi4Δ* double mutant was nearly identical to that of *swi4Δ*, again suggesting that *Whi5* acts upstream of *Swi4* (Fig. 3B). The small

cell size caused by *prs3Δ* was almost completely unaffected by additional *cln3Δ*, *bck2Δ*, or *swi4Δ* mutations that alone cause a pronounced large cell size phenotype (Fig. 3B) (36). Thus, in the absence of *PRS3*, the canonical regulators *CLN3*, *BCK2*, and *SWI4* have almost no effect on the timing of Start. *PRS3* encodes one of five ribose-phosphate pyrophosphokinases in yeast and may be required for cell cycle arrest in response to nutrient deprivation (37). Lastly, the size of *ptk2Δ cdh1Δ* double mutants was indistinguishable from that of the *cdh1Δ* single mutant, suggesting that *CDH1* may act downstream of *PTK2* in the same pathway (Fig. 3B). These crosses also uncovered a number of synthetic genetic interactions between some *whi* mutants (Fig. 2A), such as between *sfp1Δ* and *sch9Δ*, which may therefore converge on the same essential process.

Given the paucity of epistatic interactions between established Start pathways and our newly identified cell size regulators, it seems likely that uncharacterized pathways control the critical cell size threshold. A major pathway appears to involve aspects of ribosome biogenesis. Deletion of any of five nonessential genes implicated in ribosome biogenesis, *RPA14*,

**Fig. 3. Genetic epistasis reveals a network of pathways that regulate Start. (A)** *Whi* strains were tested for size epistasis with deletions of known Start regulators (*cln3Δ*, *bck2Δ*, and *swi4Δ*) and a newly identified regulator (*cdh1Δ*). Pairwise genetic interactions: +, additive interaction; arrows, epistatic interactions pointing to the dominant deletion; ND, not determined; —, synthetic lethal interaction; C, more complex size phenotype. Most *prs3Δ* spores germinated into very slow-growing colonies and were not analyzed. The *whi6Δ swi4Δ* double mutant was larger than the *swi4Δ* single mutant. The *sch9Δ cdh1Δ* double mutant was larger than *sch9Δ* but smaller than *cdh1Δ*. *KAP122* and *CDH1* are tightly linked on chromosome VII, so double mutants were not isolated. **(B)** Informative epistatic interactions for cell size distributions, as labeled with arrows. **(C)** Essential genes involved in ribosome biogenesis couple cell growth to cell division. Cell size was plotted as a function of doubling time. Open triangles, haploinsufficient *whi* mutants deleted for essential genes involved in ribosome biogenesis; closed squares, wild-type control and haploinsufficient *whi* mutants deleted for essential genes that encode ribosome subunits deleted; gray circles, a heterozygous *sch9Δ/SCH9* strain. Error bars indicate one standard deviation for both axes.



REPORTS

*RPA49*, *SSF1*, *SKY1*, and *TOM1*, caused substantial decreases in cell size without a proportionate decrease in growth rate (triangles in Fig. 2B, Table 1). Heterozygous deletion in any of 10 essential genes involved in ribosome biogenesis caused decreases in cell size but with less severe increases in doubling time than those caused by heterozygous deletions in essential subunits of the ribosome (table S2, Fig. 3C). Thus, the reduction in cell size caused by defects in ribosomal biogenesis appears not to be solely a consequence of reduced growth rate.

Expression of 11 of 15 of the size control genes implicated in ribosome biogenesis depended on Sfp1. Not only was the *sfp1Δ*

strain one of the smallest *whi* mutants recovered, overexpression of *SFP1* resulted in very slow growth and a Lge phenotype (36). To determine the direct transcriptional targets of Sfp1, an *sfp1::GALI-SFP1* strain was shifted from raffinose to galactose medium, and the consequences of restoring *SFP1* expression was monitored by DNA microarray analysis over time (*t*). (26). Shortly after *SFP1* induction, expression of 116 genes was evident; of these, 73 fell into the discrete functional categories of nucleotide biosynthesis, transfer RNA synthetases, ribosome biogenesis, ribosomal RNA (rRNA) transcription, and translation initiation and elongation (Fig. 4A, *t* = 30 min). Of the remaining 43 genes, 21 encoded proteins that form multiple interactions

within a nucleolar protein network. After induction of the initial gene set, nearly all of the genes encoding ribosomal proteins (RPs) were collectively induced (Fig. 4A, *t* = 50 min). All of the gene clusters induced by *SFP1* were repressed in an *sfp1Δ* strain (Fig. 4A). Many genes implicated in ribosome biogenesis are transcriptionally coregulated, probably through two promoter elements termed RRPE and PAC (38, 39). The set of Sfp1-regulated early genes was enriched for RRPE and PAC elements, which thus represent candidate binding sites for Sfp1 (Fig. 4A). *RP* gene promoters did not contain RRPE and PAC elements, whereas Sfp1-regulated early gene promoters did not contain binding sites for Rap1 (40), a transcriptional

**Table 1.** Characterization of *whi* mutants. Strains at or below the growth rate–cell size baseline as defined in Fig. 2B are listed in order of increasing size; ± 1 SD is reported for each parameter. All strains listed here showed tight linkage between *kanR*-marked gene deletion and the *Whi* phenotype. Homologs have 25% amino acid identity over more than half the protein, except

for SPAC22G7.02 and importin 13, which only have ~20% identity. *R*, resistance; *S*, sensitivity to mating pheromone α-factor, relative to the response of the wild-type strain (*WT*) (26). ORF overlaps between *YGR064W* and *SPT4* and between *YNL227C*, *YNL226W*, and *YNL228W* preclude definitive assignment of the *Whi* phenotype. NA, not applicable.

Deleted gene	Doubling time (min)	Haploid cell size (fl)		1N DNA content (%)	% budded	Resist.	Heterozygote cell size (fl)		Known role	Homolog(s)	
		Daughter	Median				Daughter	Median		<i>S. pombe</i>	Human
<i>SFP1</i> †	220 ± 17	8 ± 1	25 ± 1	73 ± 0	24 ± 4	<i>S</i>	46 ± 2	76 ± 1	Unknown	SPAC16.05c	
<i>SCH9</i> †	153 ± 2	9 ± 1	28 ± 1	64 ± 3	43 ± 2	<i>S</i>	40 ± 4	69 ± 2	Growth control	Sck1/2	Akt1/2/3 (PKB)
<i>PRS3</i> †	135 ± 3	17 ± 1	30 ± 1	44 ± 1	65 ± 2	<i>S</i>	47 ± 2	79 ± 4	Nucleotide metabolism	SPCC1620.06*	
<i>WHI3</i>	108 ± 3	17 ± 0	31 ± 1	42 ± 2	57 ± 7	<i>R</i>	48 ± 1	77 ± 4	Localizes <i>CLN3</i> mRNA	Prps1/2*	
<i>WHI5</i> †	88 ± 2	18 ± 0	32 ± 1	34 ± 4	68 ± 7	<i>R</i>	52 ± 2	90 ± 3	Unknown		
<i>RPA49</i>	137 ± 8	16 ± 1	33 ± 1	57 ± 6	44 ± 7	<i>S</i>	47 ± 3	78 ± 2	rRNA transcription	Rpa49	FLJ13390
<i>YNL227C</i>	124 ± 9	16 ± 1	34 ± 1	50 ± 2	42 ± 5	<i>WT</i>	45 ± 0	73 ± 2	Unknown	SPAC6B12	08
<i>YNL226W</i>	126 ± 11	16 ± 1	34 ± 1	52 ± 4	45 ± 4	<i>WT</i>	45 ± 0	74 ± 2	Unknown		
<i>PHO5</i>	125 ± 3	17 ± 0	34 ± 1	46 ± 0	49 ± 1	<i>WT</i>	43 ± 1	71 ± 1	Acid phosphatase	Pho1	
<i>HXK2</i>	86 ± 4	19 ± 0	34 ± 1	51 ± 6	59 ± 3	<i>WT</i>	49 ± 3	81 ± 3	Glucose signaling	Hxk1*	Hk1*
<i>YHR034C</i>	111 ± 7	18 ± 0	35 ± 0	61 ± 1	38 ± 6	<i>WT</i>	50 ± 4	84 ± 3	Unknown		FLJ20643
<i>SKY1</i> †	97 ± 4	18 ± 0	35 ± 1	52 ± 1	47 ± 7	<i>WT</i>	49 ± 2	80 ± 3	SR protein kinase	Dsk1	Srpk1
<i>KAP122</i> †	91 ± 1	19 ± 1	35 ± 1	52 ± 4	53 ± 6	<i>WT</i>	51 ± 5	84 ± 4	Nuclear transport	SPAC22G7.02	importin 13
<i>SSF1</i> †	107 ± 8	18 ± 0	36 ± 1	53 ± 1	41 ± 6	<i>WT</i>	52 ± 1	82 ± 4	Nucleolar protein	SPAC6B12.01	Ppan
<i>RPA14</i> †	97 ± 2	19 ± 0	36 ± 1	48 ± 2	61 ± 5	<i>WT</i>	53 ± 6	85 ± 8	rRNA transcription		
<i>YGR111W</i>	103 ± 6	19 ± 0	36 ± 1	46 ± 1	56 ± 2	<i>WT</i>	51 ± 2	84 ± 5	Unknown		
<i>YCR061W</i>	91 ± 1	19 ± 1	36 ± 1	45 ± 2	57 ± 10	<i>WT</i>	45 ± 2	77 ± 1	Unknown		
<i>PTK2</i> †	88 ± 3	20 ± 1	36 ± 1	46 ± 1	45 ± 2	<i>WT</i>	51 ± 0	83 ± 0	Protein kinase		
<i>TOM1</i>	99 ± 0	18 ± 0	37 ± 1	44 ± 2	57 ± 2	<i>WT</i>	45 ± 1	71 ± 2	Ubiquitin-protein ligase	SPAC19D5.04	
<i>GPA2</i> †	91 ± 6	20 ± 0	37 ± 0	55 ± 7	53 ± 12	<i>WT</i>	50 ± 4	82 ± 5	cAMP signaling	Gpa2*	Gnai1*
<i>KEL1</i>	87 ± 4	21 ± 0	37 ± 1	42 ± 1	62 ± 7	<i>WT</i>	52 ± 1	82 ± 3	Cell polarity	Tea1	
<i>SWE1</i>	91 ± 2	19 ± 0	38 ± 1	49 ± 1	50 ± 1	<i>WT</i>	50 ± 4	83 ± 3	Inhibitory kinase	Wee1	Wee1
<i>YGR064W</i>	91 ± 1	21 ± 1	39 ± 1	41 ± 2	69 ± 1	<i>WT</i>	53 ± 2	84 ± 2	Unknown		
<i>CDH1</i> †	115 ± 4	14 ± 2	40 ± 1	35 ± 3	64 ± 6	<i>S</i>	51 ± 5	89 ± 7	Cyclin degradation	Srw1	hCdh1
<i>WHI6</i> †	102 ± 5	19 ± 0	43 ± 3	50 ± 2	52 ± 3	<i>R</i>	50 ± 3	84 ± 1	Unknown		
<i>WT</i>	87 ± 6	23 ± 0	42 ± 2	44 ± 1	59 ± 5	<i>WT</i>	50 ± 2	82 ± 0	NA	NA	NA

\*Proteins that belong to members of highly conserved families with multiple *S. pombe* and/or human homologs. †Strains subjected to epistasis analysis.

REPORTS

activator of *RP* genes (Fig. 4A). On the basis of the kinetics of gene induction, one or more Sfp1-regulated genes may cue Rap1 to express *RP* genes in a transcriptional cascade that ultimately controls both critical cell size and ribosome biogenesis.

The nucleolus is the site of ribosome construction, in which rRNA is transcribed, processed, and assembled into ribosomes (41). Ribosome assembly is thought to be mediated by large macromolecular factories; as an organelle, the nucleolus is defined not by membranes but by protein-RNA, protein-DNA, and protein-protein interactions (41). Of the 15 factors implicated in cell size control and ribosome biogenesis, 13 are components of a large network highly enriched in nucleolar proteins, as defined by large-scale protein interaction data sets (26). This nucleolar network may contain up to 250 proteins, depending on how the network is defined. We assembled a subnetwork containing the 13 cell size control proteins and 106 other highly connected proteins (Fig. 4B). Of these 119 factors, 59 have been implicated in ribosome biogenesis (31), 46 have been localized to the yeast nucleolus (31), and 39 are homologs of proteins found in purified human

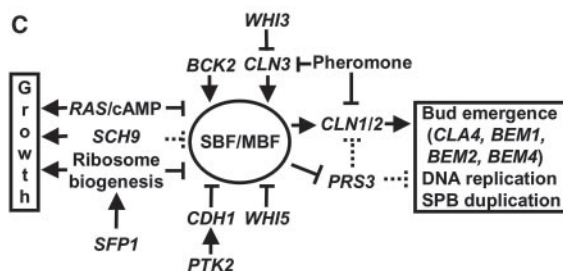
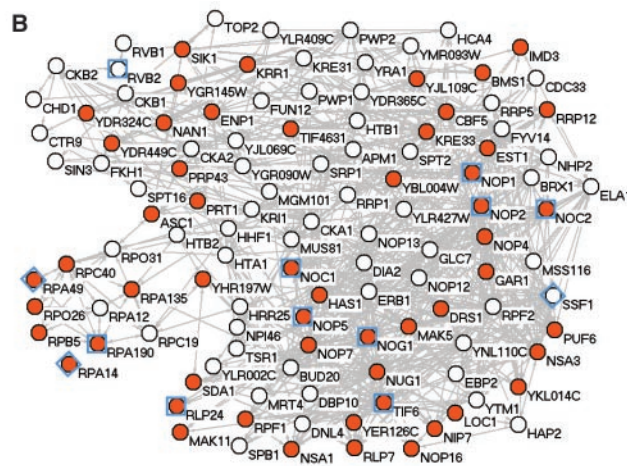
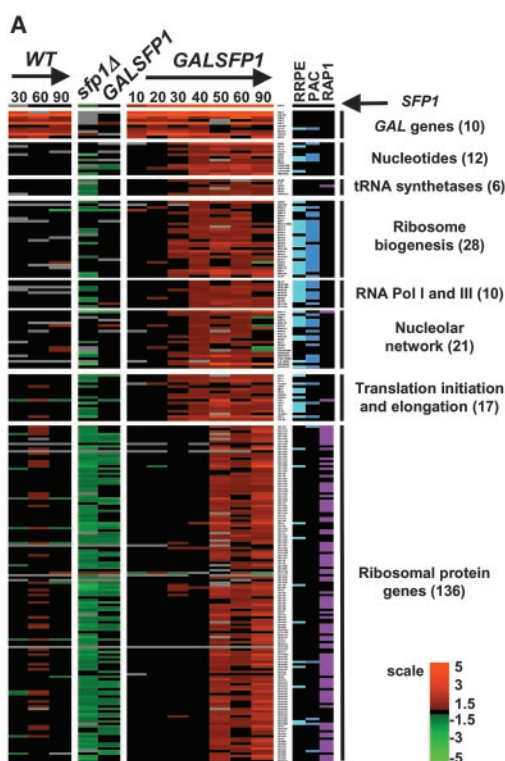
nucleoli (42). About half of this network was controlled at the level of Sfp1-dependent transcription (red dots, Fig. 4B).

The above synthetic lethal interactions, epistatic relations, and DNA microarray data identify and partially order pathways that establish the critical cell size threshold at Start (Fig. 4C). The conventional pathway for activation of Start includes Cln3-Cdc28 and Bck2, which trigger the  $G_1$ -S gene expression program by activating the SBF and MBF transcription factors. Our genomewide analysis suggests that up to 40 previously unidentified components also control Start, many of which are implicated in ribosome biogenesis (Fig. 4C). Of the newly identified Start regulators that we have studied, *WHI5*, *CDH1*, and *SFP1* appear to act upstream of SBF and MBF but not through Cln3 and Bck2 (Figs. 2C and 3A). *Whi5* does not have similarity to other known proteins, but it is expressed in a  $G_1$ -periodic manner (22), consistent with a role at Start. On the basis of its known biochemical role as a substrate recruitment factor for the APC/C (33), *Cdh1* may target one or more activators of Start for ubiquitin-dependent proteolysis. Amongst the factors im-

plicated in ribosome biogenesis, Sfp1 is the most potent repressor of Start, presumably because it controls the expression of numerous genes that influence cell size.

The partial uncoupling of growth from division by specific mutations in ribosome biogenesis pathways suggests that the critical cell size threshold is not set simply as a passive downstream readout of protein synthetic rate (43). Instead, commitment to division may be dynamically linked to signals that stimulate ribosome biogenesis, which is the predominant biosynthetic activity of a growing yeast cell (44). That is, the cell may anticipate changes in its protein synthetic rate by adjusting the critical cell size threshold before any actual change in ribosome content. This interpretation is consistent with the observation that the critical cell size threshold increases in nutrient-rich conditions, as do the rates of ribosome biogenesis and protein synthesis (6, 44). Although the nature of the repressive influence of ribosome biogenesis on Start remains to be determined, the interplay between ribosome assembly and cell cycle progression appears to be a conserved feature of eukaryotic cell division (14, 45, 46). In the absence of S6K, which stimulates growth

**Fig. 4.** Sfp1 controls expression of a nucleolar network that is enriched in cell size control genes. (A) DNA microarray analysis revealed Sfp1-dependent expression of 94 genes in the indicated functional classes. Congenic wild-type and *sfp1::GAL1-SFP1* strains grown in rich medium containing 2% raffinose were induced with 2% galactose and were harvested at the indicated time points (min). Expression ratios relative to the initial raffinose culture are shown for each time point. Red indicates >1.5-fold increase (induction), green indicates <1.5-fold decrease (repression), and gray signifies that no reliable measurement was obtained. The transcriptional profile of cells lacking Sfp1 was determined by comparing raffinose-grown *sfp1::GAL1-SFP1* versus WT strains (*GAL1-SFP1* column) or glucose-grown *sfp1Δ::kanR* versus WT strains (*sfp1Δ* column). Genes induced early in the *sfp1::GAL1-SFP1* time course contained strong matches to upstream RRPE (light blue) and PAC (dark blue) promoter elements but not RAP1 elements, which activate *RP* gene transcription (purple). The number of genes in each functional class is indicated in parentheses. For an enlarged version of Fig. 4A, see fig. S3. (B) Thirteen cell size control genes implicated in ribosome biogenesis are embedded in a nucleolar protein interaction network. Interactions between proteins encoded by



13 cell size control genes (squares, 10 haploinsufficient *whi* strains from Fig. 3C; diamonds, 3 *whi* strains Table 1) and 106 of the most highly interconnected proteins, as determined from large-scale coimmunoprecipitation data, are shown in a binary representation (26). Gene names are to the lower right of each node. Transcriptional targets of Sfp1 are indicated by red circles. (C) Summary of cell size control genes that act at Start. Epistatic interactions were assumed to reflect linear pathways, but parallel pathways are also formally possible. Dashed lines indicate uncertain interactions. Genes that were not ordered are not shown.

by activating the translation of ribosomal components, fly cells become abnormally small (14, 45). Pathways that control critical cell size at Start in budding yeast may provide further insight into mechanisms that couple growth and division in higher organisms.

References and Notes

1. T. P. Neufeld, B. A. Edgar, *Curr. Opin. Cell Biol.* **10**, 784 (1998).
2. L. H. Hartwell, J. Culotti, J. R. Pringle, B. J. Reid, *Science* **183**, 46 (1974).
3. F. R. Cross, *Curr. Opin. Cell Biol.* **7**, 790 (1995).
4. G. C. Johnston, J. R. Pringle, L. H. Hartwell, *Exp. Cell Res.* **105**, 79 (1977).
5. R. K. Mortimer, *Radial. Res.* **9**, 312 (1958).
6. G. C. Johnston, C. W. Ehrhardt, A. Lorincz, B. L. Carter, *J. Bacteriol.* **137**, 1 (1979).
7. P. Nurse, *Nature* **256**, 547 (1975).
8. J. G. Umen, U. W. Goodenough, *Genes Dev.* **15**, 1652 (2001).
9. D. Killander, A. Zetterberg, *Exp. Cell Res.* **40**, 12 (1965).
10. A. Yen, J. Fried, T. Kitahara, A. Stride, B. D. Clarkson, *Exp. Cell Res.* **95**, 295 (1975).
11. I. J. Conlon, G. A. Dunn, A. W. Mudge, M. C. Raff, *Nature Cell Biol.* **3**, 918 (2001).
12. S. A. Backman *et al.*, *Nature Genet.* **29**, 396 (2001).
13. C. H. Kwon *et al.*, *Nature Genet.* **29**, 404 (2001).
14. S. C. Kozma, G. Thomas, *Bioessays* **24**, 65 (2002).
15. P. E. Sudbery, A. R. Goodey, B. L. Carter, *Nature* **288**, 401 (1980).
16. R. Nash, G. Tokiwa, S. Anand, K. Erickson, A. B. Futcher, *EMBO J.* **7**, 4335 (1988).
17. F. R. Cross, *Mol. Cell. Biol.* **8**, 4675 (1988).
18. E. Gari *et al.*, *Genes Dev.* **15**, 2803 (2001).
19. M. Tyers, G. Tokiwa, B. Futcher, *EMBO J.* **12**, 1955 (1993).
20. R. S. Nash, T. Volpe, B. Futcher, *Genetics* **157**, 1469 (2001).
21. C. J. Di Como, H. Chang, K. T. Arndt, *Mol. Cell. Biol.* **15**, 1835 (1995).
22. P. T. Spellman *et al.*, *Mol. Biol. Cell* **9**, 3273 (1998).
23. H. Wijnen, B. Futcher, *Genetics* **153**, 1131 (1999).
24. E. A. Winzeler *et al.*, *Science* **285**, 901 (1999).
25. Cultures were grown in rich media containing 2% glucose at 30°C to 0.3 to 3 × 10<sup>7</sup> cells/ml, a range in which wild-type size distributions do not vary. Cell clumps were dispersed with a sonicator, and size distributions were obtained with a Coulter Channelizer Z2 (Beckman-Coulter).
26. Materials and methods are available as supporting material on Science Online.
27. M. B. Eisen, P. T. Spellman, P. O. Brown, D. Botstein, *Proc. Natl. Acad. Sci. U.S.A.* **95**, 14863 (1998).
28. B. J. Breitkreutz, P. Jorgensen, A. Breitkreutz, M. Tyers, *Genome Biol.* **2** (2001).
29. Before hierarchical clustering of haploid deletion strains, each size distribution (10 to 128 fl) was normalized as a percentage of total counts and then smoothed by averaging over a seven-bin sliding window.
30. A. H. Y. Tong *et al.*, *Science* **294**, 2364 (2001).
31. Gene functions can be found at the Saccharomyces Genome Database, available at <http://genome-www.stanford.edu/Saccharomyces/>.
32. C. B. Tyson, P. G. Lord, A. E. Wheals, *J. Bacteriol.* **138**, 92 (1979).
33. J. M. Peters, *Curr. Opin. Cell Biol.* **10**, 759 (1998).
34. Z. Xu, D. Norris, *Genetics* **150**, 1419 (1998).
35. P. Fabrizio, F. Pozza, S. D. Pletcher, C. M. Gendron, V. D. Longo, *Science* **292**, 288 (2001).
36. P. Jorgensen, J. Nishikawa, M. Tyers, unpublished data.
37. K. M. Binley, P. A. Radcliffe, J. Trevethick, K. A. Duffy, P. E. Sudbery, *Yeast* **15**, 1459 (1999).
38. C. Wade, K. A. Shea, R. V. Jensen, M. A. McAlear, *Mol. Cell. Biol.* **21**, 8638 (2001).
39. J. D. Hughes, P. W. Estep, S. Tavazoie, G. M. Church, *J. Mol. Biol.* **296**, 1205 (2000).
40. J. D. Lieb, X. Liu, D. Botstein, P. O. Brown, *Nature Genet.* **28**, 327 (2001).
41. T. Melese, Z. Xue, *Curr. Opin. Cell Biol.* **7**, 319 (1995).
42. J. S. Andersen *et al.*, *Curr. Biol.* **12**, 1 (2002).

43. M. Polymenis, E. V. Schmidt, *Curr. Opin. Genet. Dev.* **9**, 76 (1999).
44. J. R. Warner, *Trends Biochem. Sci.* **24**, 437 (1999).
45. J. Montagne *et al.*, *Science* **285**, 2126 (1999).
46. R. J. White, *Trends Biochem. Sci.* **22**, 77 (1997).
47. We thank B. Andrews, A. Tong, C. Boone, H. Bussey, K. Chan, and C. Y. Ho for providing reagents; C. Stark for programming; and G. Bader, A. Amon, L. Harrington, B. Andrews, D. Durocher, and Y. Masui for comments on the manuscript. P.J. holds a Canadian Institutes of Health Research (CIHR) Studentship, J.N. holds an Ontario Graduate Scholarship, and M.T. holds a Canada Research Chair in Biochemistry. Supported by grants to M.T. from the National Cancer Institute of

Canada with funds from the Terry Fox Foundation, the CIHR, the Canada Foundation for Innovation, and the Ontario Innovation Trust.

Supporting Online Material

[www.sciencemag.org/cgi/content/full/1070850/DC1](http://www.sciencemag.org/cgi/content/full/1070850/DC1)  
Materials and Methods

Figs. S1 to S3  
Tables S1 and S2

13 February 2002; accepted 4 June 2002

Published online 27 June 2002;

10.1126/science.1070850

Include this information when citing this paper.

## Serotonin Transporter Genetic Variation and the Response of the Human Amygdala

Ahmad R. Hariri,<sup>1</sup> Venkata S. Mattay,<sup>1</sup> Alessandro Tessitore,<sup>1</sup> Bhaskar Kolachana,<sup>1</sup> Francesco Fera,<sup>1</sup> David Goldman,<sup>2</sup> Michael F. Egan,<sup>1</sup> Daniel R. Weinberger<sup>1\*</sup>

A functional polymorphism in the promoter region of the human serotonin transporter gene (*SLC6A4*) has been associated with several dimensions of neuroticism and psychopathology, especially anxiety traits, but the predictive value of this genotype against these complex behaviors has been inconsistent. Serotonin [5-hydroxytryptamine, (5-HT)] function influences normal fear as well as pathological anxiety, behaviors critically dependent on the amygdala in animal models and in clinical studies. We now report that individuals with one or two copies of the short allele of the serotonin transporter (5-HTT) promoter polymorphism, which has been associated with reduced 5-HTT expression and function and increased fear and anxiety-related behaviors, exhibit greater amygdala neuronal activity, as assessed by BOLD functional magnetic resonance imaging, in response to fearful stimuli compared with individuals homozygous for the long allele. These results demonstrate genetically driven variation in the response of brain regions underlying human emotional behavior and suggest that differential excitability of the amygdala to emotional stimuli may contribute to the increased fear and anxiety typically associated with the short *SLC6A4* allele.

The elucidation of underlying biological mechanisms that contribute to individual differences in both normal and abnormal behavior remains a crucial and largely unmet challenge. Advances in both molecular genetics and noninvasive functional neuroimaging, however, have begun to address this issue, particularly in regards to affective behaviors, such as fear and anxiety, which exhibit considerable individual variability (1). In humans, two common alleles, the short (s) and long (l), in a variable repeat sequence of the

promoter region of the serotonin transporter gene (5-HTTLPR) have been differentially associated with anxiety-related behavioral traits in healthy subjects (2, 3). Likewise, both positron emission tomography and functional magnetic resonance imaging (fMRI) studies have revealed links between the physiological responses of brain regions, such as the prefrontal cortex and amygdala, and individual differences in affect and temperament (4, 5).

At the physiological level, the serotonin transporter promoter polymorphism alters both *SLC6A4* transcription and level of serotonin transporter function. Cultured human lymphoblast cell lines homozygous for the l allele have higher concentrations of 5-HTT mRNA and express nearly twofold greater 5-HT reuptake compared with cells possessing either one or two copies of the s allele, which may act dominantly (2). Nearly identical differences in 5-HTT binding levels in human brain were detected between individuals with the l/l versus l/s or s/s genotypes,

<sup>1</sup>Clinical Brain Disorders Branch, Intramural Research Program, National Institute of Mental Health, National Institutes of Health, Bethesda, MD 20892, USA. <sup>2</sup>Laboratory of Neurogenetics, Intramural Research Program, National Institute on Alcohol Abuse and Alcoholism, National Institutes of Health, Bethesda, MD 20892, USA.

\*To whom correspondence should be addressed at Clinical Brain Disorders Branch, National Institute of Mental Health, 10 Center Drive, Room 4S235, Bethesda, MD 20892-1384, USA. E-mail: weinberd@intra.nimh.nih.gov



## Systematic Identification of Pathways That Couple Cell Growth and Division in Yeast

Paul Jorgensen *et al.*  
*Science* **297**, 395 (2002);  
DOI: 10.1126/science.1070850

*This copy is for your personal, non-commercial use only.*

**If you wish to distribute this article to others**, you can order high-quality copies for your colleagues, clients, or customers by [clicking here](#).

**Permission to republish or repurpose articles or portions of articles** can be obtained by following the guidelines [here](#).

**The following resources related to this article are available online at [www.sciencemag.org](http://www.sciencemag.org) (this information is current as of October 9, 2015 ):**

**Updated information and services**, including high-resolution figures, can be found in the online version of this article at:

<http://www.sciencemag.org/content/297/5580/395.full.html>

**Supporting Online Material** can be found at:

<http://www.sciencemag.org/content/suppl/2002/07/18/1070850.DC1.html>

A list of selected additional articles on the Science Web sites **related to this article** can be found at:

<http://www.sciencemag.org/content/297/5580/395.full.html#related>

This article has been **cited by** 238 article(s) on the ISI Web of Science

This article has been **cited by** 100 articles hosted by HighWire Press; see:

<http://www.sciencemag.org/content/297/5580/395.full.html#related-urls>

This article appears in the following **subject collections**:

Cell Biology

[http://www.sciencemag.org/cgi/collection/cell\\_biol](http://www.sciencemag.org/cgi/collection/cell_biol)